

# Progress in the Development and Performance of a High Frequency 4 K Stirling-Type Pulse Tube Cryocooler

P.E. Bradley, R. Radebaugh, I. Garaway, and E. Gerecht

National Institute of Standards and Technology  
Boulder, Colorado, 80305, USA

## ABSTRACT

Presently we are in the development process for a 4 K Stirling-type pulse tube cryocooler to support cooling requirements for a mobile THz detector system. In this paper we discuss the status of this development and the optimization methods for achieving 4 K with a three-stage hybrid design employing separate He-4 first and second stages that precool a He-3 third-stage. Acoustic power is provided by a linear compressor operating at 60 Hz and 2.5 MPa for the He-4 cryocoolers, whereas, a separate linear compressor operating at 30 Hz and 1.0 MPa provides acoustic power for the He-3 cryocooler. The first stage regenerator employs stainless steel mesh while the second stage regenerator employs erbium-praseodymium (ErPr). The third stage regenerator is layered with gadolinium oxysulphate (GOS) spheres at the cold end and erbium-praseodymium (ErPr) spheres at the warm end. This hybrid modular cryocooler design allows for a modular optimization approach for each cryocooler that mitigates time consuming redesign and fabrication of unaffected stages during the cryocooler development. Progress for each stage development and performance (goals and measured) optimization are presented.

## INTRODUCTION

While many technologies benefit from a stable low temperature ( $<10$  K), most would further benefit from efficient, compact, high frequency Stirling-type pulse tube cryocoolers. Pulse tube cryocoolers operating at sufficiently high frequencies, on the order of 30 Hz or higher, can deliver reduced vibration, compact size, and improved efficiency over currently available Gifford-McMahon and GM-type pulse tube cryocoolers that operate at 1-2 Hz. They also can reduce the loss of the dwindling supply of helium while eliminating the difficult logistics of liquid helium cryostats. This further maintains or even reduces the overall system size and footprint. Presently we are undertaking an effort to develop a 4 K pulse tube cryocooler that supports a program to develop a mobile THz detection system (known as a mobile demonstrator). Figure 1 shows a schematic of the laboratory-based system upon which the mobile system is based<sup>1,2</sup>. The present laboratory system relies on a GM cryocooler for the 4 to 5 K needed. Use of a GM cryocooler presents distinct challenges. The GM displays higher than desirable temperature fluctuation, high vibration at low frequency, sizable input power ( $\sim 5$  kW), and requires water heat rejection from the compressor. The goal of this effort is to improve cooler performance (temperature stability and efficiency) while reducing size and power to such levels that enable a mobile system.

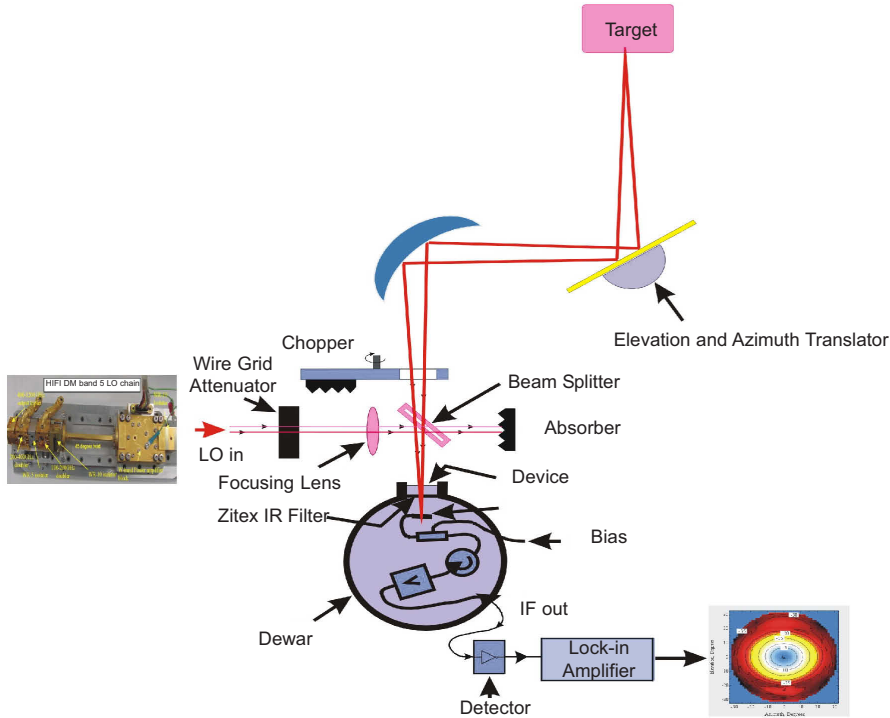


Figure 1. Schematic of Terahertz imaging system.

PULSE TUBE CRYOCOOLER – STATUS

The cryocooler is an important enabling technology for this mobile THz demonstrator. The pulse tube cryocooler under development uses a multistage split gas approach employing three stages similarly to Olson, et al.<sup>3,4</sup>. There are three stages in the low pressure, 1 MPa He-3 pulse tube that has the first and second stage precooled by the high pressure, 2.5 MPa He-4 pulse tube. Separate pressure oscillators are used for each of the two gases. The He-4 pulse tube takes gas from the pressure oscillator and splits flow between a single-stage pulse tube to intercept 80 K losses from radiation (300 K to 80 K) and electrical leads, and a separate second-stage pulse tube to intercept He-3 second-stage losses and precool the He-3 third stage to 25 K. Ordinarily He-4 would be employed for a cooler of this nature. However, recent use of He-3 in low frequency GM–type pulse tube cryocoolers<sup>5,6</sup> and discussions by Radebaugh<sup>7</sup> and Kittel<sup>8</sup> lay considerable merit for its use in the third stage for temperatures below 10 K. The high cost of He-3 (~\$1K/std. liter and climbing) is outweighed by the performance improvement especially for a separate, small 4 to 5 K stage as this cooler requires.

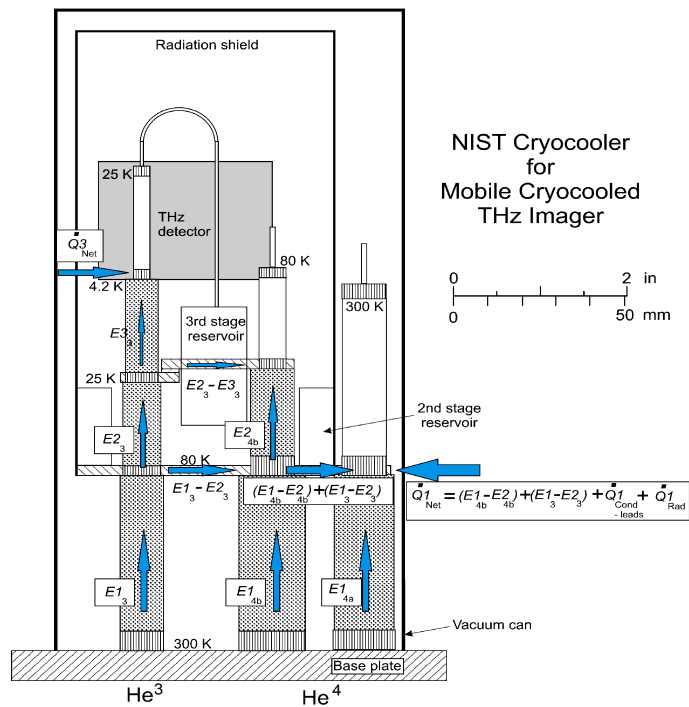
Cooler requirements derive from heat loads at the terahertz detector, detector leads, and self-cooling loads of the cryocooler. Operating loads and cooler design parameters<sup>9</sup> are summarized in Tables 1 and 2. Figure 2 shows a schematic for the three stage pulse tube emphasizing modularity

Table 1. Pulse tube design and operating parameters.

	Pulse Tube					
	V, cm <sup>3</sup>	Q <sub>net</sub> , W	PV input, W	Operating Frequency, Hz	Operating Charge Pressure, MPa	Operating Pressure Ratio
He-4, 1 <sup>st</sup> stage	5.84	20	200	60	2.5	1.25
He-4, 2 <sup>nd</sup> stage	2.15	2.3	270	60	2.5	1.20
He-3, 3 <sup>rd</sup> stage	0.96	0.050	260	30	1.0	1.5

**Table 2.** Regenerator geometries and materials.

	300-80K, Regenerator			80-25K, Regenerator			25-4 K, Regenerator		
	$\phi_{ID}$ , cm	$V$ , cm <sup>3</sup>	Material	$\phi_{ID}$ , cm	$V$ , cm <sup>3</sup>	Material	$\phi_{ID}$ , cm	$V$ , cm <sup>3</sup>	Material
He-4, 1 <sup>st</sup> stage	1.86	13.61	#400 SS Screen	n/a					
He-4, 2 <sup>nd</sup> stage	2.17	18.5	#400 SS Screen	1.84	8.0	Er <sub>0.5</sub> Pr <sub>0.5</sub> 100 $\mu$ m spheres	n/a		
He-3, 3 <sup>rd</sup> stage	2.19	12.63	#200 SS Screen	1.56	2.17	Er <sub>0.5</sub> Pr <sub>0.5</sub> 100 $\mu$ m spheres	1.47	5.1	GOS + Er <sub>0.5</sub> Pr <sub>0.5</sub> 100 $\mu$ m spheres



**Figure 2.** Staging configuration for multi-stage split gas pulse tube cryocooler. Modular performance verification is emphasized using this approach. Blue arrows represent heat flows.

while Fig. 3 shows the CAD rendering for the pulse tube cryocooler and terahertz mixer. Performance evaluation/verification for each stage may be undertaken sequentially by first evaluating the first stage, then adding the second, and finally the third. This modularity allows us to evaluate loads at each stage by employing an energy balance as shown in Fig. 2. Presently, we are in process of evaluating performance of the first stage. The second stage components are complete and ready for final braze assembly in preparation for performance evaluation. A concurrent evaluation of the third stage pulse tube and regenerator (not including 1<sup>st</sup> and 2<sup>nd</sup> precooling regenerators) has been constructed and is undergoing evaluation in a separate vacuum test fixture utilizing a GM to pre-cool the stage to ~25 to 30 K. Garaway et al.<sup>10</sup> present thorough results for this testing with He-3 and He-4 as the working fluid. While Radebaugh, et al.<sup>11</sup> also present more thorough discussion on a novel phase shift technique employed to improve pulse tube operation for near 4 K. Table 3 summarizes results for the various phase shift techniques employed.

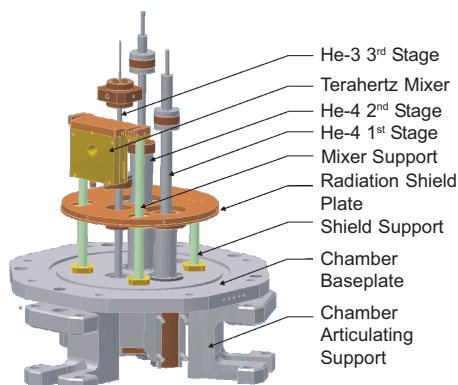


**Figure 3.** Solid rendering of multi-stage split pulse tube cooler and terahertz detector.

<u>Inertance tube</u>	
– He-4:	$T_c = 10.6\text{ K}$
– He-3:	$T_c = 7.7\text{ K}$
<u>Double Inlet (with secondary regenerator)</u>	
He-4:	$T_c = 15.8\text{ K}$
He-3:	(Not tested)
<u>Expander (<math>4\text{ cm}^3</math>) (with secondary regenerator)</u>	
– He-4:	$T_c = 6.4\text{ K}$
– He-3:	$T_c = 5.4\text{ K}$

**Table 3.** Summary of 3<sup>rd</sup> stage regenerator and pulse tube preliminary performance, precooled to  $\sim 30\text{ K}$ .

**First Stage Performance**

Performance of the first stage was evaluated using a 500 W commercial pressure oscillator intended for both first and second stages. The system has limited instrumentation which does not allow for direct measurement of the acoustic power delivered by the compressor. Thus a current limit not to exceed 10 A bounds operating conditions for input power as tested. Input powers were varied from 250 to 350 W electrical input for frequencies of 55, 60, and 70 Hz and the nominal inertance tube. The nominal design frequency is 60 Hz. However, as is customary a variation in frequency was evaluated to characterize the pulse tube-compressor coupling. Figs. 4 and 5 show the cooling at 80 K for the first stage as a function of input power and pressure ratio at the compressor. Theoretically, for the first stage, the design pressure ratio at the compressor should be  $\sim 1.35$  in order to deliver a pressure ratio of 1.25 at the pulse tube and 200 W of acoustic power. In reality we find that we need  $\sim 350\text{ W}$  or more to achieve 1.35 pressure ratio at the compressor. Furthermore, we find from Fig. 6 that the power factor (which is a percentage of the product of voltage times amperage at the ideal in phase relationship) for the compressor to cold head match is rather poor at 0.33 to 0.44 while having no dependence upon input power for a non-loaded condition. However, we do observe the power factor varying directly with increasing frequency and a dependence upon cold head load in Fig. 7. This suggests rather strong correlation of an imbalance of cold head impedance to that of the compressor. Essentially, we have a poor impedance match between the compressor and cold head as lower values correspond with poor resonance conditions. We would expect values of around .75 to 1.0 for good resonance operation.

The 1<sup>st</sup> stage achieved a low no-load temperature of  $\sim 43\text{ K}$  for the nominal design of 60 Hz with the nominal inertance tube. Whereas, a slightly lower 41 K was achieved for 70 Hz with a

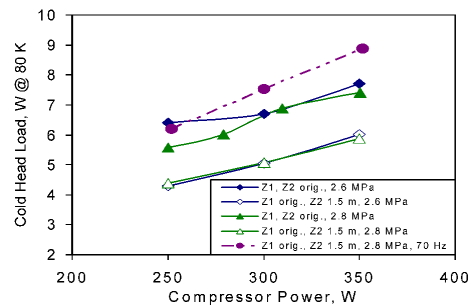


**Figure 4.** 1<sup>st</sup> stage load as a function of compressor input power.

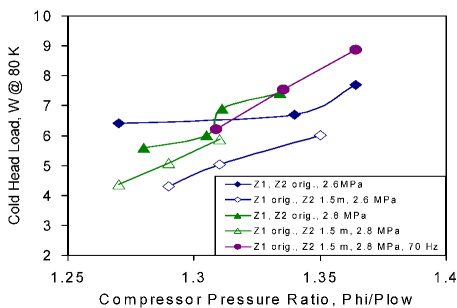


**Figure 5.** 1<sup>st</sup> stage load as a function of pressure ratio at the compressor.

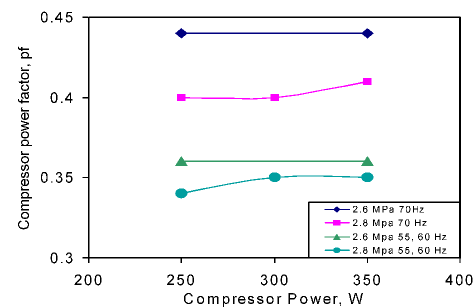


**Figure 6.** Power factor for compressor as a function of input power.

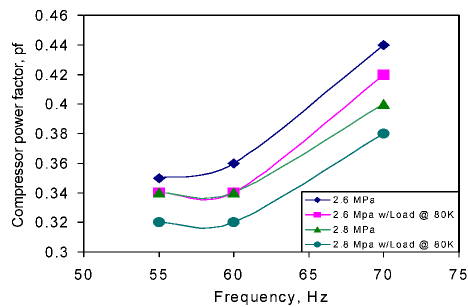


**Figure 7.** Dependence of power factor with frequency.

shorter length (1.5 m) of the large diameter inertance tube. Figure 8 shows the no-load temperatures for varying frequency and charge pressure for two different double-diameter inertance tubes tested. Lowest temperatures occur for operation at 70 Hz regardless of charge pressure. Figure 9 gives mass flows at the warm end of the pulse tube for 60 Hz operation, as measured from amplitudes in the reservoir, for varying pressure ratio at the compressor. For the second double-diameter inertance tube combination the mass flow more closely resembles expected values of  $\sim 1.7$  g/s. However, this occurs for higher pressure and frequency than the nominal design. This corresponds with a higher load capacity at 80 K as expected.

In Fig. 10 we compare estimated acoustic power delivered by the compressor with electrical power input. As stated previously the cold head is not instrumented to obtain the acoustic power at the cold head. Therefore we are left only with the input power or perhaps in this case the estimated acoustic power determined from scaling laws for pressure oscillators and information provided by the compressor manufacturer<sup>12</sup>. Essentially, 350 W input or even slightly more are required to deliver less than 200 W of acoustic power to the cold head validating the impedance mismatch. Radebaugh et al.<sup>13</sup>, recently discussed the importance of this impedance matching between cold head and compressor and the significance to overall efficiency of both compressor and cold head performance. Due to poor 1<sup>st</sup> stage performance of considerably lower cooling of  $\sim 8$  W at 80 K compared to desired values of  $\sim 18$  W a background heat leak test was performed as shown in Fig. 11. It resulted in a background load of 1.87 W which compared quite favorably with calculations estimating  $\sim 1.9$  W. Thus we must explore other sources for losses in the stage to explain this poor performance. One likely candidate is the cold end heat exchanger which was shortened to 3 mm in length as a compromise to achieve adequate packaging of the cold head. From calculations for this heat exchanger we find that the gas likely is not properly maintained to near the heat exchanger temperature by as much as 15 or 20% which corresponds to a gas temperature that is as much as 3 K different from that of the heat exchanger. This then presents considerable performance degradation

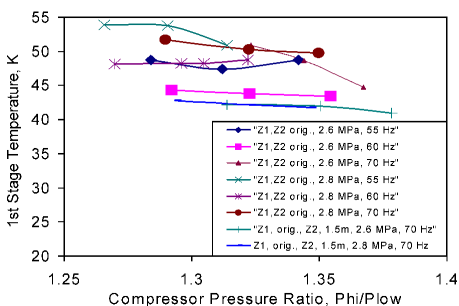


**Figure 8.** 1<sup>st</sup> stage no-load as function of frequency and charge pressure.

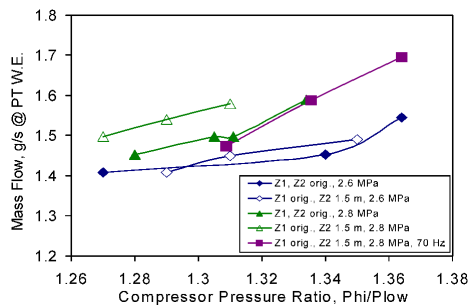


**Figure 9.** Pulse tube warm end mass flows for 60 Hz operation with cold end @ 80 K.

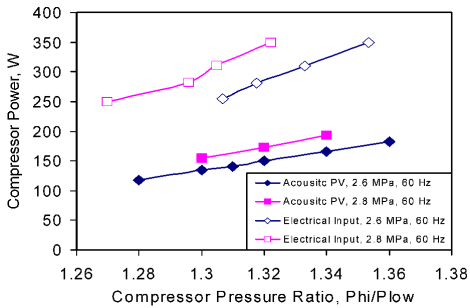


**Figure 10.** Pressure ratio as a function of estimated acoustic power.

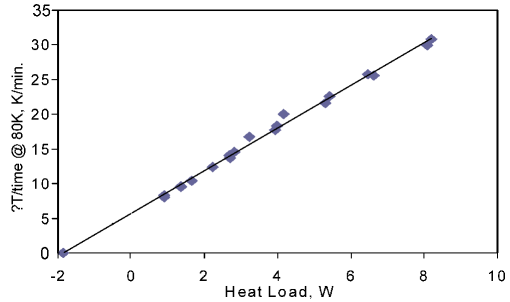


**Figure 11.** Background heat leak.

which must therefore be intercepted in the pulse tube which in turn can lead to further reduction in the efficiency of the pulse tube.

## CONCLUSION

Performance evaluation of the first and third stages of a multistage split gas pulse tube cryocooler has commenced. The second stage evaluation is close to initiation which may alleviate some impedance mismatch between the first stage cold-head and compressor. Further evaluation of the first stage is needed to improve the net cooling to necessary levels to support precooling of the second and third stage in addition to radiation from 300 K.

## ACKNOWLEDGMENTS

We gratefully acknowledge financial and moral support from NIST in this endeavor.

## REFERENCES

1. Gerecht, E., Gu, D., You, L., and Yngvesson, K. S., "A passive heterodyne hot electron bolometer imager operating at 850 gigahertz," *IEEE Trans. Micr. Theory Tech.*, vol. MTT56, pp. 1083-1091, May 2008.
2. Gu, D., Gerecht, E., Rodriguez-Morales, F., and Yngvesson, S., "Two-Dimensional Terahertz Imaging System Using Hot Electron Bolometer Technology", *17th Intern. Symp. Space THz Technol.*, Paris, France, April 10-12, 2006.
3. Olson, J., "Development of a 4.5 K Pulse Tube Cryocooler for Superconducting Electronics," *Adv. in Cryogenic Engineering*, Vol. 53, Amer. Institute of Physics, Melville, NY (2008), pp. 881-886.
4. Olson, J., "Development of Remote Cooling Systems for Low-Temperature, Space-Borne Systems", *Cryocoolers 14*, ICC Press, Boulder, CO 2007, pp. 33-40.
5. Xu, M.Y., de Waele, A.T.A.M., Ju, Y.L., "A pulse tube refrigerator below 2 K," *Cryogenics* 39 (1999), pp.865-869.
6. Jiang, N., Lindemann, F., Giebeler, F., and Thummes, G., "A 3He pulse tube cooler operating down to 1.3 K," *Cryogenics* 44 (2004), pp. 809-816.
7. Radebaugh, R., Huang, Y. H., O'Gallagher, A., and Gay, J., "Calculated Regenerator Performance at 4 K with Helium-4 and Helium-3," *Adv. in Cryogenic Engineering*, Vol. 53, Amer. Institute of Physics, Melville, NY (2008), pp. 225-234.
8. Kittel, P., "Performance Limits of Pulse Tube Cryocoolers using  $^3\text{He}$ ," *Adv. in Cryogenic Engineering*, Vol. 53, Amer. Institute of Physics, Melville, NY (2008), pp. 1421-1428.

9. Bradley, P.E., Gerecht, E., Radebaugh, R., and Garaway, I., "Development of a 4 K Stirling-Type Pulse Tube Cryocooler for a Mobile Terahertz Detection System," *Adv. in Cryogenic Engineering*, Vol. 55, Amer. Institute of Physics, Melville, NY (2010), pp. 1593-1600.
10. Garaway, I., Lewis, M., Bradley, P., and Radebaugh, R., "Measured and Calculated Performance of a High Frequency, 4 K Stage, He-3 Regenerator," *Cryocoolers 16*, ICC Press, Boulder, CO (2011), (this proceedings).
11. Radebaugh, R., O'Gallagher, A., and Gary, J., "Secondary Pulse Tubes and Regenerators for Coupling to Room-Temperature Phase Shifters in Multistage Pulse Tube Cryocoolers," *Cryocoolers 16*, ICC Press, Boulder, CO (2011), (this proceedings).
12. Marquardt, E., Radebaugh, R., and Kittel, P., "Design equations and scaling laws for linear compressors with flexure springs," *Proc. 7<sup>th</sup> International Cryocooler Conference*: Air Force Report PL-CP-93-1001, (1993), pp. 783-804.
13. Radebaugh, R., Garaway, I., and Veprik, A., "Development of Miniature, High Frequency Pulse Tube Cryocoolers", to be published in *Proceedings of SPIE*, Vol. 7660, 2010.

